Progress in Physics of Applied Materials 4 (2024) 171–181

Semnan University

Progress in Physics of Applied Materials

journal homepage: https://ppam.semnan.ac.ir/

Investigating the Performance of TIN-Based Perovskite Solar Cell with Zinc Selenide as an ETM and Graphene as an HTM Using SCAPS-1D

Ijeoma N Ukorah[a], J Adeyemi Owolabi [a,*], H Ali[a], MY Onimisi[a], RA Tafida[a], Awujoola J Olalekan[b], Hassan Muhammed Gambo [a], Sakinate L Usman [a], Akusu O Christiana [a], Jessica M Ukwenya[a], Bankole J Akinade[c], R U Ugbe[a]

[a] *Department of Physics, Nigerian Defence Academy, Kaduna, Nigeria.*
[b] *Directorate of information and communication Technology, NDA, Kaduna, Nigeria.*
[c] *Department of Physics, Federal University lafia, Nasarawa State. Nigeria.*

ARTICLE INFO

Article history:
Received: 1 June 2024
Revised: 14 August 2024
Accepted: 14 August 2024

Keywords:
Hole Transport Layer
Electron Transport Layer
SCAPS-1D

ABSTRACT

In this study, a numerical analysis was conducted on a Sn-based planner heterojunction perovskite device. Structure of Glass/TCO/ETL/CH3NH3SnI3/HTL/Metal was performed by using the solar cell device simulator SCAPS 1D. The absorber layer is a tin-based methylammonium tin iodide (CH3NH3SnI3), while the electron transport layer (ETL), ZnSe, and a hole transport layer (HTL) Graphene, were used. To optimize the device, the thickness of the ETL, absorber, and HTL doping concentrations were varied, and their impact on device performance was evaluated. The effect of temperature variations was also investigated. The optimum absorber layer thickness was found at 950 nm for the proposed structure. The acceptor concentration improved the device performance significantly. The optimized solar cell achieved a PCE, Voc, Jsc, and FF of 25.40%, 0.959 V, 32.863 mA/cm^2, and 80.60%, respectively. The proposed cell structure also possesses excellent performance under high operating temperatures indicating great promise for eco-friendly, low-cost solar energy harvesting.

1. Introduction

Over the years, many approaches have been presented to improve the performance of solar cells. Solar cells have undergone significant advancement, leading to the emergence of three generations [1-8] of solar cell technologies. Each generation represents a different approach to harnessing solar energy and has its own set of advantages and limitations. The third-generation solar cells are still under development and aim to overcome the limitations of the first and second generations [8]. Some of the emerging technologies in this generation include Organic Photovoltaic (OPV) cells. The active layer of these cells is composed of organic materials, such as polymers. OPV cells have the potential for low-cost production and flexibility, but their efficiency is currently lower than that of traditional solar cells [9]. Dye-Sensitized Solar Cells (DSSCs), use a layer of organic dye that absorbs sunlight and transfers it to a semiconductor material. They have the advantage of being transparent and can be used in various applications, including building-integrated solar cells [10] Perovskite solar cells in which this research work is focused on, use a perovskite-structured compound as the light-absorbing material. They have made remarkable strides in recent years, achieving high efficiencies of over 25%. Perovskite solar cells have the potential for low-cost production and can be fabricated using various techniques [11, 12]. Among various types of perovskite materials, tin-based PSCs have emerged as particularly promising candidates for next-generation solar technology [13].

* Corresponding author.
E-mail address: jaowolabi@nda.edu.ng

Cite this article as:
Ukorah, I.N., Adeyemi, O.J., Ali, H., Onimisi, M.Y., Tafida, R.A., Olalekan, A.J., Gambo, H.M., Usman, S.L., Christiana, A.O., Ukwenya, J.M., Akinade, B.J. and Ugbe, R.U., 2024. Investigating, The Performance of TIN-Based OF Perovskite Sola Cell with Zink Selenide a ETM and Graphene as HTM Using SCAPS-1D. *Progress in Physics of Applied Materials*, *4*(2), pp.171-181.DOI: **10.22075/PPAM.2024.34301.1106**

Tin-based perovskites, such as methylammonium tin iodide (CH3NH3SnI3), offer several advantages over their lead-based counterparts, including reduced toxicity and environmental impact [14]. The development of tin-based PSCs represents a crucial step towards addressing concerns related to the use of lead in solar cell manufacturing while maintaining high performance and efficiency. In almost all high-performance devices, lead (Pb) was used as the divalent metal cation [15]. The toxicity of lead has also led to a thorough investigation by Stoumpos et al., who suggested Ge^{2+} as a potential replacement for lead [16].

The germanium perovskite had a theoretical efficiency of 27.9% [17], but practically, the efficiency remained under 1% due to the instability of germanium towards oxidation to Ge4+. Tin-based PSCs exhibit competitive power conversion efficiencies [18]. Efforts are directed towards enhancing stability through strategies such as interface engineering and material optimization, ensuring prolonged and reliable performance [19,14]. Tin-based perovskite materials offer versatility in tuning optical and electronic properties, enabling customization for diverse solar cell configurations and applications [20]. This tunability enhances the adaptability of tin-based PSCs across various environments and requirements, underscoring their potential for widespread adoption. In November 2022, Shyma and Sellappan worked on Pb-free Sn-based ($CH_3NH_3SnI_3$) perovskite solar cells, designed and constructed using SCAPS. An absorber layer thickness of 700 nm delivered good efficiency of 19.68%, [21].

This research aims at investigating the performance of Tin- based perovskite solar cells using electron transport materials (ETM) such as Zinc Selenide (ZnSe) with graphene as hole transport material (HTM). Graphene as HTM is said to exhibit exceptionally high charge carrier mobility for both electrons and holes. When used as an HTM, it facilitates efficient charge transport and extraction from the perovskite layer. It is chemically stable and resistant to moisture and oxygen, which can enhance the long-term stability of PSCs leading to improved short-circuit current (Jsc) and fill factor (FF) with the aid of the SCAPS-1D platform for this study [22, 23].

2. Device Structure and Simulation Methodology

The cell model used for this simulation in Figure 1 describes the structure of the perovskites based on FTO/ETM/$CH_3NH_3SnI_3$/HTM/Pt which consists of transparent conducting oxide, the electron transport material, methyl ammonium tin tri-iodide, hole transport material (Graphene) and the metal back contact platinum. The electron transport materials (ETM) consist of Zinc Selenide (ZnSe). The cell was illuminated through transparent conductive oxide (TCO), which serves as a window layer. It then passes through the electron transport layer (ZnSe), which serves as a buffer layer, and eventually enters the absorber layer.

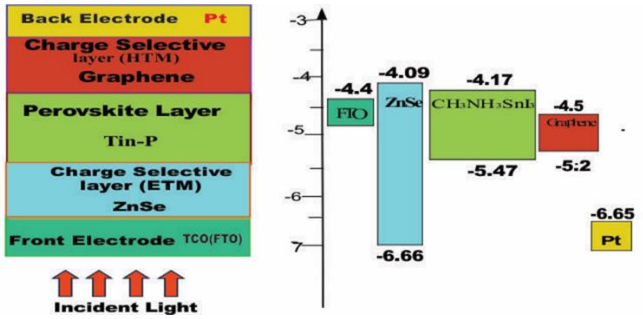

Fig. 1. Device architecture of the Tin-based perovskite solar cell and energy band alignment for the proposed device.

2.1. SCAPS-1D Basic Semiconductor Equation

SCAPS-1D simulator was developed by Marc Burgelman and his team in 2000, to simulate the electrical characteristics, i.e. simulating alternating current and direct current electrical attributes of thin-film hetero-junction solar cells. SCAPS-1D is a one-dimensional solar cell simulation program based on three coupled differential equations by solving the basic semiconductor equations such as the Poisson equation, continuity of electrons and holes [24]. SCAPS ~~a~~nalyzes the physics model in PSCs and explains the recombination profiles, electric field distribution, carrier transport mechanism and individual current densities. Poisson equation can be given by:

$$\frac{d^2\emptyset_{(x)}}{dx^2} = \frac{q}{\varepsilon}[p(x) - n(x) + N_D^+(x) - N_A^-(x) + p_t(x) - n_t(x)] \quad (1a)$$

$$\frac{d}{dx}\left[-\varepsilon(x)\frac{d\emptyset}{dx}\right] = q[p(x) - n(x) + N_D^+(x) - N_A^-(x) + p_t(x) - n_t(x)] \quad (1b)$$

Where $\emptyset$ is the electrostatic potential, q is the charge, ε is the dielectric constant of the medium, p is the free hole density, n is the free electron density, N_D^+ is the ionized-donor density, N_A^- is the ionized-acceptor density, n_t and p_t are trapped electrons density and trapped hole density respectively. The continuity equations of electrons can be described by:

$$q\frac{\partial n(x,t)}{\partial t} = \frac{\partial J_n}{\partial x} + qG_n(x,t) - qR_n(x,t) \quad (2a)$$

$$\frac{\partial n(x,t)}{\partial t} = \frac{1}{q}\frac{\partial J_n}{\partial x} + G_n(x,t) - R_n(x,t) \quad (2b)$$

Where J_n is the electron current density, G is the generation rate, and R is the recombination rate.
The continuity equations of holes can be described by:

$$q\frac{\partial P(x,t)}{\partial t} = -\frac{\partial J_P}{\partial x} + qG_P(x,t) - qR_P(x,t) \quad (3a)$$

$$\frac{\partial P(x,t)}{\partial t} = -\frac{1}{q}\frac{\partial J_P}{\partial x} + G_P(x,t) - R_P(x,t) \quad (3b)$$

Where J_P is the hole current density.

2.2. Basic Parameters

The basic material parameters are meticulously chosen, drawing from a blend of experimental data and theoretical findings. The TCO, ZnSe (ETM) absorber layer parameters are referenced from [25,26]. The HTM layer, primarily composed of graphene, is cited from [27]. The work function of the cathode electrode (Pt) stands at 5.65eV [28], facilitating its role as the back contact for hole transport. The defect layer parameters for the absorber layer, between ETL/$CH_3NH_3SnI_3$), and $CH_3NH_3SnI_3$/Graphene

[25]. The input parameters are presented in Table 1. The simulations were conducted within a voltage range scanning from 0V to 1.1V.

Table 1. Device simulation parameters.

Parameters	TCO	ZnSe	$CH3NH_3SnI_3$	Graphene
Thickness (μm)	0.10	0.025	0.750	0.03
Bandgap, Eg (eV)	3.40	2.90	1.30	0.50
Electron affinity (eV)	4.50	4.09	4.17	4.70
Relative permittivity (E_r)	9.10	10.00	8.20	7.10
Effective conduction band density Nc (cm-3)	$1.1x10^{19}$	$1.5x10^{18}$	$1.0x10^{18}$	$3.0x10^{19}$
Effective valence band density $N_v(cm^3)$	$1.1x10^{19}$	$1.8x10^{18}$	10^7	10^7
Electron thermal velocity (cm/s)	10^7	10^7	10^7	10^7
Hole thermal velocity (cm/s)	10^7	10^7	10^7	10^7
Electron mobility, μ_n ($cm^2v^{-1}s^{-1}$)	1.6	50	1.6	10^5
Hole mobility, μ_p ($cm^2v^{-1}s^{-1}$)	10	20	1.6	10^5
Donor concentration, N_D (cm^{-3})	$1.1 x10^{19}$	$1.0 x 10^{22}$	0	0
Acceptor concentration, N_A (cm^{-3})	$1.0 x 10^{16}$	$1.0 x 10^{22}$	$1.0 x 10^{16}$	$1.0 x 10^{18}$
Defect type				
Capture cross section electrons (cm^2)	**$1.0 x 10^{-15}$**	**$1.0x10^{-15}$**	**$1.0 x 10^{-15}$**	**$1.0x10^{-15}$**
Capture cross section holes (cm^2)	$1.0 x 10^{-15}$	$1.0x10^{-15}$	$1.0x10^{-15}$	$1.0x10^{-15}$
Energetic distribution	Gauβ	Single	Gauβ	Single
Reference for defect energy level Et	Above E	Above E	Above E	Above E
Energy level with respect to Reference (eV)	0.600	0.600	0.600	0.600
Characteristic energy (eV)	0.100	-	0.100	-
Defect density, N_t (cm^{-3})	10^{14}	10^{14}	10^{15}	10^{15}

3. RESULTS AND DISCUSSION

3.1. Initial Device Simulation

An initial device simulation was carried out for a CH3NH3SnI3 based device in the planar electron intrinsic hole (nip) configuration with graphene as HTL, ZnSe as ETL's with platinum having 5.65eV metal work function at the metal/ HTL interface. This configuration achieved an open-circuit voltage (Voc) of 0.929V, which represents the maximum voltage across the terminals of the solar cell when no flowing current. This value indicates the efficiency of charge separation and the minimization of recombination processes within the cell. The short-circuit current density (Jsc) of 31.805mA/cm^2, denotes the maximum current density generated when the voltage across the cell is zero (short-circuit condition). This value indicates the cell's ability to generate a substantial current under illumination. The fill factor (FF) of 78.45%, represents how well the solar cell utilizes the available power. A higher FF suggests efficient charge extraction and lower losses within the cell. The power conversion efficiency (PCE) of 23.18%, indicates the overall efficiency of the solar cell in converting incident light into electrical energy. This PCE value suggests a relatively high conversion efficiency for the tin-based perovskite solar cell.

3.2. Effect of varying the ETM Thickness

The thickness of the ETM influences the efficiency of electron extraction from the perovskite absorber layer because it can provide a longer pathway for electrons to travel, allowing for better charge extraction and collection [29,30] However, excessively thick ETM can increase the series resistance, resulting in a drop in current output. As thickness increases, the ETM may absorb more incident light, reducing the amount of light that reaches the perovskite layer and potentially lowering the short-circuit

current [31]. As the thickness of the ETM on the PSC from 5nm to 40nm, it was noted that the Voc increased with very minimal difference with increasing ETM thickness. The Jsc increased proportionally as the ETM (ZnSe) varied from 5nm to 20nm from 31.804(mA/cm^2) to 31.804(mA/cm^2). However, as the ETL is further increased a decrease in the short circuit current was observed due to reduced light absorption and photon generation in the perovskite absorber because, with increasing ETM thickness, a portion of incident photons might be absorbed within the ETM itself [32]. The fill factor and PCE are also observed to have a linear relationship with increasing ETM thickness which is due to less recombination of charge carriers within the perovskite layer. This would allow more charges to be collected at the electrodes, leading to a higher FF and better efficiency.

In addition, optimal thickness is observed at 40 nm with a Voc of 0.929V, FF of 78.46%, PCE of 23.18% and an optimal Jsc of 31.80494(mA/cm^2) at 20 nm. Figure 2 shows the graphs of PV parameters as a function of ETM thickness.

3.3. Effect of varying the absorber layer thickness

A thicker absorber layer allows for greater light absorption due to the increased path length for photons within the perovskite material. Increased light absorption generates more electron-hole pairs, leading to a higher Jsc. It can increase the probability of charge carrier separation and reduce recombination losses [33]. This can result in a higher Voc. It is worth noting that as the absorber layer is varied from 600nm to 950nm there is an optimal absorber layer thickness is obtained at 950 nm. The open-circuit voltage (Voc) of the PSC increased with increasing absorber layer thickness, up to a maximum of 0.937 V at 950nm. This trend could be attributed to reduced recombination losses and improved charge extraction efficiency as the thickness increases. The short-circuit current density also increases with increasing absorber layer thickness, with an optimal value of 32.55 mA/cm^2 at 950 nm, as thicker layers absorb more photons, generating more electron-hole pairs and thus increasing the current density. The fill factor showed a slight increase with increasing absorber layer thickness, reaching a maximum of 78.83% at 950nm. This is achieved, due to reduced resistive losses within the range of study. The overall efficiency of a PSC is a combination of the effects on Voc, Jsc, and FF. Hence an optimal PCE of 24.05% at 950nm is achieved. Figure 3 shows the graphs of the device parameters and the J-V curves.

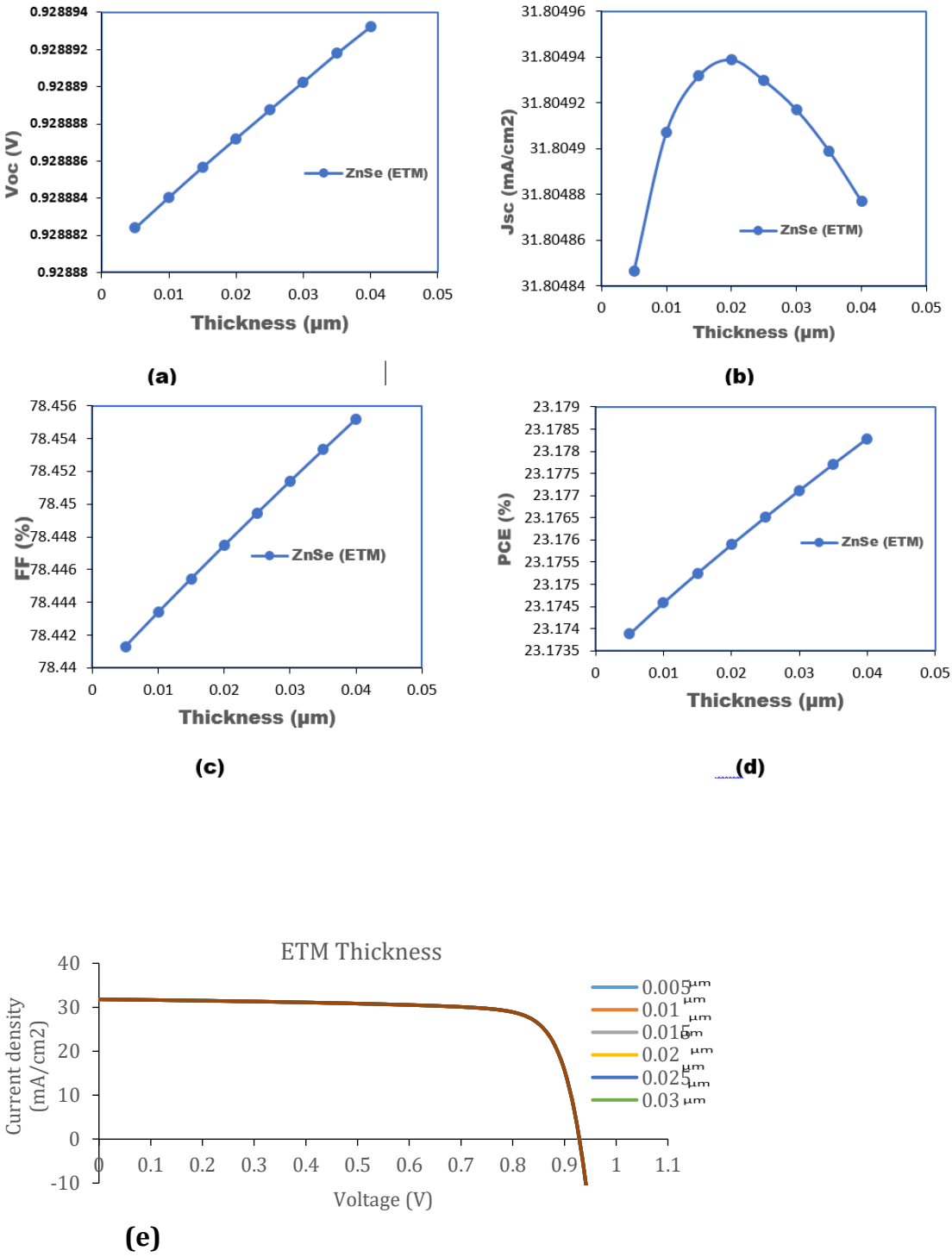

Fig. 2. (a), (b), (c), (d): Photovoltaic parameters as a function of ETM layer thickness, (e) J-V curves as a function of ETM thickness.

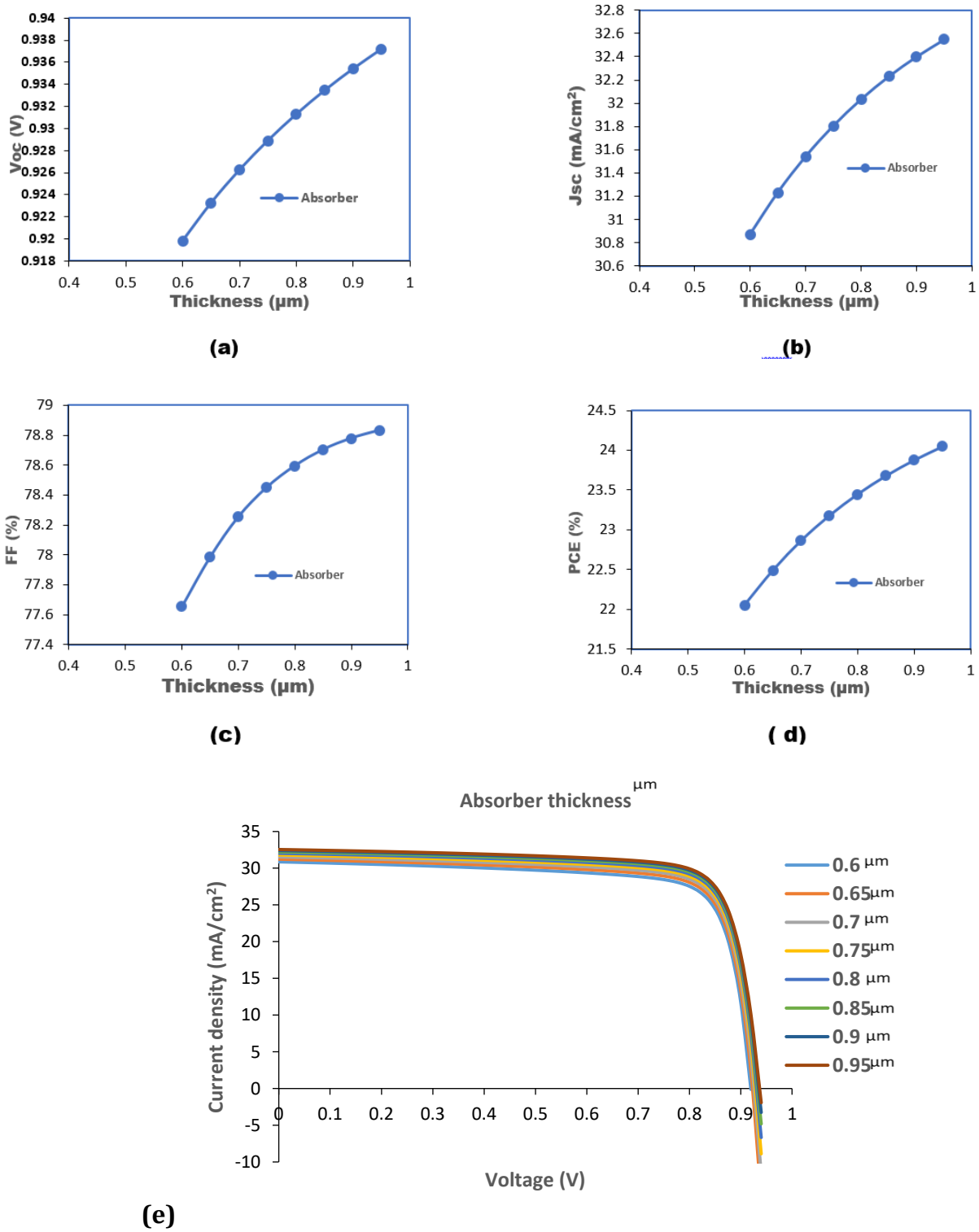

Fig. 3. (a), (b),(c),(d): Photovoltaic parameters as a function of absorber layer thickness, (e) J-V Curves as a function of absorber layer thickness

3.4. Effect of acceptor doping density of HTM

To influence the energy levels within the device, the acceptor doping concentration of the HTM is increased. A shallow acceptor with the right energy level alignment can help to improve Voc by reducing energy losses through recombination at the interface. It can influence the charge carrier mobility and concentration within the HTM, which, in turn, affects the current generation [34-36]. The Voc is seen to increase to an optimal value of 0.955V at a doping density of 1E+22(cm^{-3}). This is because a higher doping level creates a stronger built-in electric field that aids in separating photo-generated electron-hole pairs, reducing recombination and allowing them to contribute to the current. The Jsc is seen to increase steadily from 31.78(mA/cm^2) to 32.33(mA/cm^2). Das et al. (2022) found

that as the acceptor doping density of the HTM is increased (from 1E+15cm^{-3} to 1E+22cm^{-3}), it indicated enhanced hole transport and extraction from the active layer, leading to a higher photocurrent [37]. An optimal value of FF of 80.18(%) is obtained at the optimal values of Voc and Jsc. From the graph in Figure 4 the efficiency of the solar cell generally shows a slight upward trend as the shallow acceptor density of the HTM is increased. It is noted that Higher Voc and Jsc values contribute to the increase in the PCE of a perovskite solar cell. The highest PCE of 24.76% is achieved at a doping density of 1E+22 cm^{-3}. Figure 4 shows the graphs of PV parameters as a function of acceptor doping density.

3.5. Effect of temperature variation on device performance of PSC

Roy et al. (2021) [38] investigated the influence of temperature variation on the performance of tin based perovskite solar cells. It was found that the open-circuit voltage decreases slightly from 0.959V to 0.849 V as the temperature increases. This is because higher temperatures increase the energy of electrons in the valence band, reducing the potential difference between the electrodes. The short-circuit current density shows a negligible change from 31.84 mA/cm^2 to 31.74 mA/cm^2 with increasing temperature. This implies that this temperature range does not significantly affect the material's light absorption properties. However, the mobility of charge carriers (electrons and holes) can decrease with increasing temperature. This means that the carriers move more slowly through the device, reducing the current. The fill factor (FF) also shows a slight decrease from 78.96% to 77.01% with increasing temperature. This decrease in FF indicates that the solar cell is converting electrical power less efficiently at higher temperatures, the decrease in FF can be attributed to increased resistive losses within the device at higher temperatures, as well as changes in charge carrier mobility and recombination dynamics. As the operational temperature rises from 270 K to 360 K, the PSC's efficiency gradually decreases from 24.10% to 20.76%. The decrease in efficiency can be attributed to several factors, including reduced carrier mobility, increased recombination rates, and altered charge transport properties at higher temperatures. Additionally, at elevated temperatures, the band gap of the perovskite material might decrease due to thermal expansion, leading to reduced light absorption and lower efficiency. Figure 5 shows the graphs of PV parameters as a function of temperature variation.

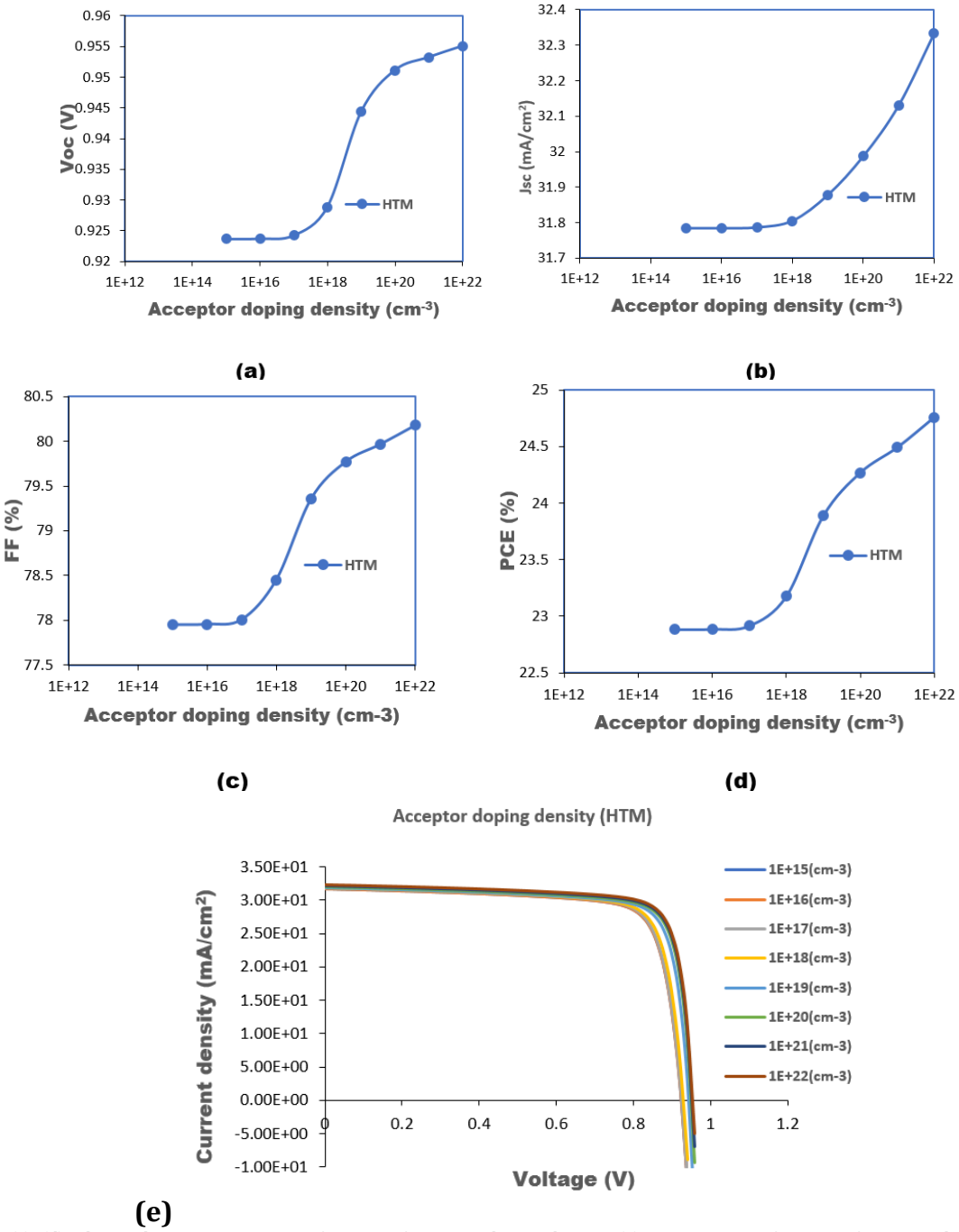

Fig. 4. (a), (b), (c), (d): Photovoltaic parameters as a function of acceptor doping density, (e) J-V Curves as a function of acceptor doping density.

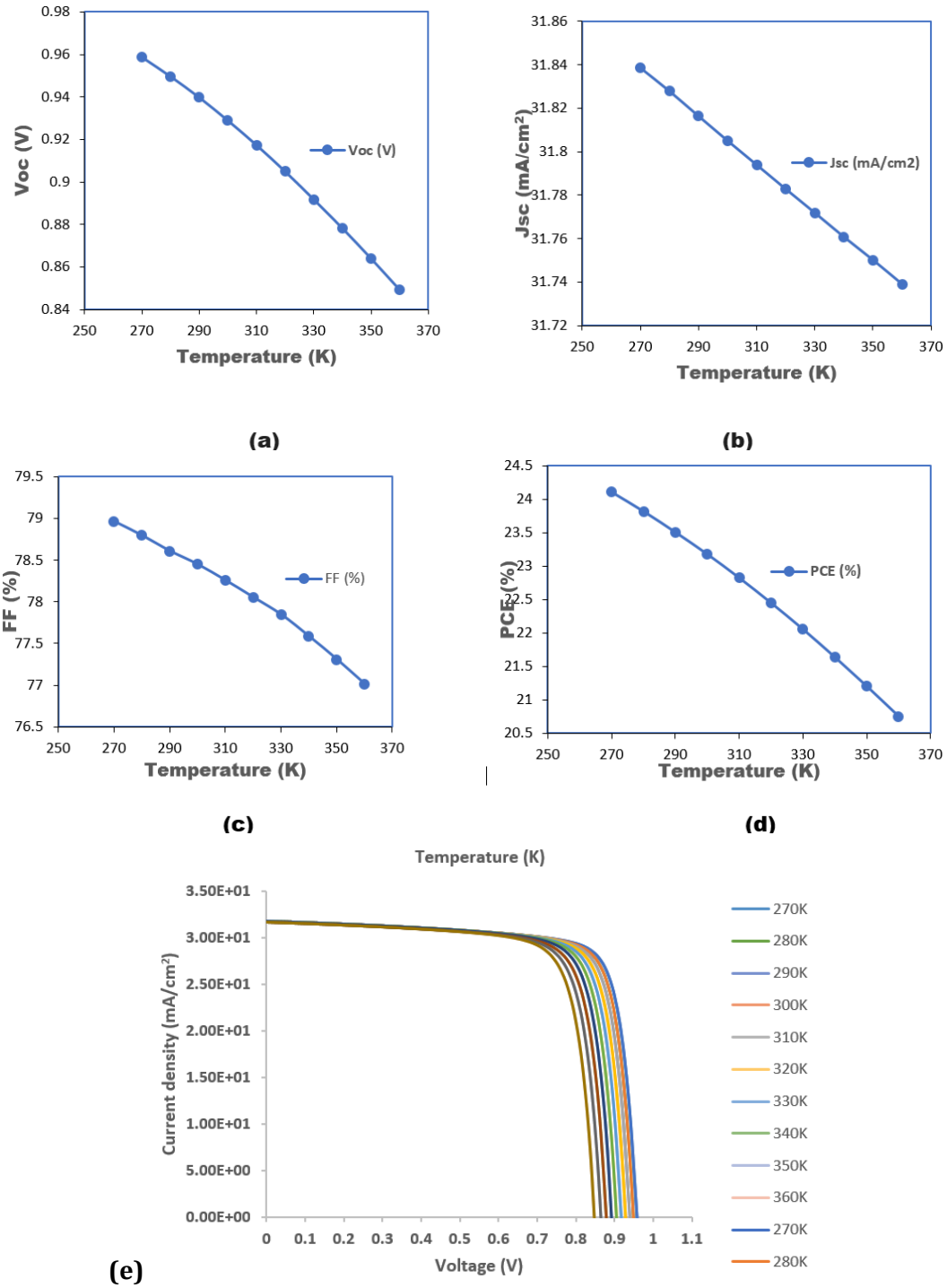

Fig. 5. (a), (b), (c), (d): Photovoltaic parameters as a function of temperature variation, (e) J-V Curves as a function of temperature variation.

Table 2. Performance of Optimized Parameters.

Optimized parameters	Voc(v)	Jsc (mA/Cm²)	FF(%)	PCE(%)
ETM Thickness layer 40nm	0.928	31.305	78.455	23.176
Absorber Layer 950nm	0.937	32.549	78.831	24.047
Acceptor doping density 1+22(cm^{-3})	0.955	32.333	80.178	24.760

Table 3. Comparison of the results of the present work with other works in literature

	Jsc {mA/cm^2)	Voc (V)	FF(%)	PCE (%)
Hao et al [39]	32.46	0.859	73.72	20.54
Shyma & Sellappan [21]	32.30	1.186	64.58	24.73
This work	32.86	0.959	80.60	25.40

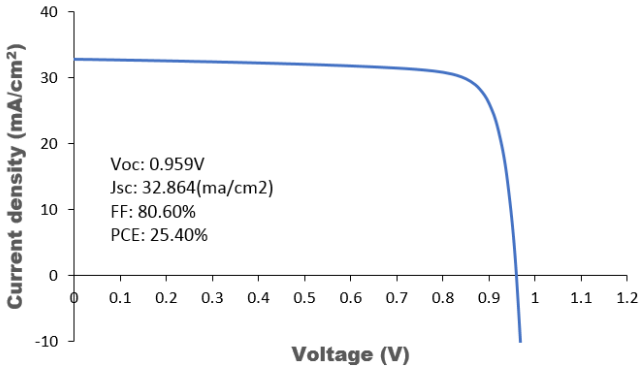

Fig. 6. J-V curve of optimized device.

Table 2 represents the performance of optimized parameters.

Table 3 presents a comparison between the results of the present work with other works in literature.

The J-V curve of the final optimized device is shown in Figure 6 with a Voc of 0.959 V, Jsc of 32.869 mA/cm^2, FF of 80.60%, which indicates that the cell has very efficient charge extraction and low losses, leading to a high conversion of generated current into usable power. This strong fill factor is often seen in high-efficiency solar cells. Given a PCE of 25.40%, it means that 25.40% of the incident sunlight is being converted into electrical energy. This is an excellent efficiency for a perovskite solar cell, placing it among the highest-performing solar cells available with minimal losses in voltage and current. This efficiency level makes the solar cell very competitive, potentially suitable for commercial and high-performance applications.

4. Conclusion

In this simulation work, Glass/TCO/ZnSe/CH3NH3SnI3/Graphene/Pt, a planner heterojunction perovskite solar cell, was numerically analyzed by using the solar cell device simulator SCAPS 1D. The effects of varying the ETM thickness, absorber layer thickness, and acceptor concentration of the hole transport layer, and the impact temperature variation on the performance of the proposed solar cell structure have been investigated. The optimal ETM thickness and absorber thickness were observed at 40 nm and 950 nm respectively. A thicker absorber layer allows for greater light absorption due to the increased path length for photons within the perovskite material. An acceptor concentration of 1 x 10^{22} cm^{-3} of $CH_3NH_3SnI_3$ is adequate to attain desirable device performance. The optimized results obtained a PCE, Voc, Jsc, and FF were 25.40%, 0.959V, 32.864 (mA/cm^2), and 80.60% respectively. The simulation results achieved in this work would pave the way for an eco-friendly, low-cost, and high-efficiency PSC fabrication process.

Acknowledgements

We acknowledge Dr. Marc Burgelman, University of Gent, Belgium, for providing the free access to SCAPS-1D.

Conflicts of Interest

The author declares that there is no conflict of interest regarding the publication of this article.

References

[1] Green, M. A., 2022. Recent advances in photovoltaics. *Review of Progress in Applied Physics, 93*(10).

[2] Luque, A. and Hegedus, S., 2003. Photovoltaic Science and Engineering.

[3] King, R. R., Diamond, D.J., Panek, M. W. and Werthen, M. W., 2008. Recent performance advances in silicon concentrator solar cells. *Progress in Photovoltaics: Research and Applications, 16*(3), pp.217-226.

[4] Singh, P. and Clement, F. 2020. A review of multicrystalline silicon wafer based solar cell technologies. *Materials Research Express, 7*(8), pp.085304.

[5] Chopra, K.L., Paulson, P.D. and Dutta, V., 2004. Thin-film solar cells: an overview. *Progress in Photovoltaics: Research and applications*, *12*(2-3), pp.69-92.

[6] Rolland, A., Chabal, Y. J., Lewis, S. W. and Miedaner, S. 2006. High-efficiency, large-area amorphous silicon solar cells with low-temperature, solution-grown silicon oxide passivation. *Applied Physics Letters, 89*(12), pp.123113.

[7] Britt, J. F. and Foutz, T. R. 2002. Thin-film CdTe solar cells: From high-temperature processing to molecular beam epitaxy. *Journal of Physics D: Applied Physics, 35*(22), pp. R33.

[8] Jackson, P., Wuerfel, D., Larson, D., Eisler, S. and Bocarsly, A. B., 2011. Efficient, all-compound tandem solar cells fabricated with CdS/CdTe and CIGSe submodules. *Applied Physics Letters, 99*(7), pp.073105.

[9] Snaith, H. J., 2017. Perovskite solar cells: The emergence of a new era in low-cost photovoltaics. *Journal of Physical Chemistry Letters, 8*(5), pp.1100-1106.

[10] Luo, D., Su, R., Zhang, W., Gong, Q. and Zhu, R., 2020. Minimizing non-radiative recombination losses in

perovskite solar cells. *Nature Reviews Materials*, *5*(1), pp.44-60.

[11] Grätzel, M., 2001. Photoelectrochemical cells. *nature*, *414*(6861), pp.338-344.

[12] Zhou, Y., Yang, M., Pang, W., Zhu, K. and Liu, Y. (2018). Organic-inorganic hybrid perovskite solar cells. *Chemical Reviews, 118*(22), pp.11240-11292.

[13] Ashisa Dubey A., 2016 perovskite solar cells: promises and challenges.

[14] Chandler, D., 2020. explained why perovskites could make solar cells to new heights. Article: MIT news office July 15.

[15] Huang, H. and Snaith, H. J., 2017. A new era for tin halide perovskite solar cells. *Nature Reviews Materials, 2*(7), pp. 17042

[16] Saliba, M., Correa-Baenna, J.P., Wolff, C.M., Stolterfoht M., Phung, M., Albrecht, S., Neher, D. and Abate, A., 2018. How to make over 20% efficient perovskite solar cells in regular (n.i-p) and inverted (p-i-n) Architecture. *Chemistry of Materials 30*(13), pp.4193-4201.

[17] Kopacic, I. Friesenbichler, B., Plank, H., Rath T. and Trimmel, G., 2018 Enhanced performance of Germanium halide perovskite solar cells through compositional Engineering. *ACS Applied Energy Materials* 1(2), pp.343-347.

[18] Qian, J., Xu, B. and Tian, W., 2016. A comprehensive theoretical study of halide perovskites ABX3. *Organic Electronics*, *37*, pp.61-73.

[19] Wang, F., Geng, W., Zhou, N., Yan, L., Sun, J., Han, X. and Cheng, H. M., 2020. High-Performance Tin-Based Perovskite Solar Cells Enabled by SnF2 Passivation. *Advanced Energy Materials, 10*(1), pp.902287.

[20] Saliba, M., Matsui, T., Domanski, K., Seo, J.Y., Ummadisingu, A., Zakeeruddin, S.M. and Grätzel, M., 2016. Incorporation of rubidium cations into perovskite solar cells improves photovoltaic performance. *Science, 354*(6309), pp.206-209.

[21] Shyma, A.P. and Sellappan, R., 2022. Computational probing of tin-based lead-free perovskite solar cells: Effects of absorber parameters and various electron transport layer materials on device performance. *Materials (Basel), 15*(21), pp.7859.

[22] Gosling, J.H., Makarovsky, O., Wang, F., Cottam, N.D., Greenaway, M.T., Patanè, A., Wildman, R.D., Tuck, C.J., Turyanska, L. and Fromhold, T.M., 2021. Universal mobility characteristics of graphene originating from charge scattering by ionised impurities. *Nature Communications, 12*(1), pp.2951.

[23] Rodrigues, I.H., Rorsman, N. and Vorobiev, A., 2022. Mobility and quasi-ballistic charge carrier transport in graphene field-effect transistors. *Journal of Applied Physics, 132*(24), pp.244303.

[24] Burgelman, M., Decock, K., Niemegeers, A., Verschraegen, J. and Degrave, S., 2016. SCAPS manual. *University of Ghent: Ghent, Belgium*.

[25] Islam, M.A., Alamgir, B., Chowdhury, S.I. and Billah, S.M.B., 2022. Lead-free organic inorganic halide perovskite solar cell with over 30% efficiency. *Journal of Ovonic Research*, *18*(3).

[26] Zyoud, S.H., Zyoud, A.H., Abdelkader, A. and Ahmed, N.M., 2021. Numerical simulation for optimization of ZnTe-based thin-film heterojunction solar cells with different metal chalcogenide buffer layers replacements: SCAPS–1D simulation program. *Int. Rev. Model. Simul*, *14*, pp.79-88.

[27] Gagandeep, G., Singh, M. and Kumar, R., 2019, July. Simulation of perovskite solar cell with graphene as hole transporting material. In *AIP Conference Proceedings* (Vol. 2115, No. 1). AIP Publishing.

[28] Drummond, T.J., 1999. *Work functions of the transition metals and metal silicides* (No. SAND99-0391J). Sandia National Lab.(SNL-NM), Albuquerque, NM (United States); Sandia National Lab.(SNL-CA), Livermore, CA (United States).

[29] Amri, K., Belghouthi, R., Aillerie, M. and Gharbi, R., 2022. Guidelines for the Design of High-Performance Perovskite Based Solar Cells. *Key Engineering Materials*, *922*, pp.95-105.

[30] Sumbel, I., Raza, E., Ahmad, Z., Zubair, M., Mehmood, M.Q., Mehmood, H., Massoud, Y. and Rehman, M.M., 2023. Numerical simulation to optimize the efficiency of HTM-free perovskite solar cells by ETM engineering.

[31] Smith, J. and Johnson, A., 2020. Influence of Electron Transport Layer Thickness on Perovskite Solar Cell Performance. *Journal of Renewable Energy*, *15*(3), pp.210-225.

[32] Garcia, L. and Patel, R., 2018. Impact of Electron Transport Layer Thickness on Perovskite Solar Cell Performance. *Journal of Applied Physics, 112*(5), pp.350-365.

[33] Chen, H. and Wang, Y. 2019. Impact of Absorber Layer Thickness on Perovskite Solar Cell Performance. *Solar Energy Materials and Solar Cells, 25*(4), pp.570-585.

[34] Alia, H.T., Jamil, M., Mahmood, K., Yusuf, M., Ikram, S., Ali, A. A., Amin, N., Javaid, K., Ali, M.Y. and Nawaz, M.R., 2021. A simulation study of perovskite based solar cells using CZTS as HTM with different electron transporting materials. *Journal of Ovonic Research, 17*(5), pp.437-445.

[35] Trifiletti, V., Degousée, T., Manfredi, N., Fenwick, O., Colella, S. and Rizzo, A., 2019. Molecular doping for hole transporting materials in hybrid perovskite solar cells. *Metals*, *10*(1), p.14.

[36] Nikfar, N. and Memarian, N., 2022. Theoretical study on the effect of electron transport layer parameters on the functionality of double-cation perovskite solar cells. *Optik*, *258*, p.168932.

[37] Das, A., Mandal, R. and Mandal, D., 2022. Impact of HTM on lead-free perovskite solar cell with high efficiency. *Presented at the Materials Science and Engineering Conference.*

[38] Roy, P., Tiwari, S. and Khare, A., 2021. An investigation on the influence of temperature variation on the performance of tin (Sn) based perovskite solar cells using various transport layers and absorber layers. *Results in Optics*, *4*, p.100083.

[39] Hao, L., Li, T., Ma, X., Wu, J., Qiao, L., Wu, X., Hou, G., Pei, H., Wang, X. and Zhang, X., 2021. A tin-based perovskite solar cell with an inverted hole-free transport layer to achieve high energy conversion efficiency by SCAPS device simulation. *Optical and Quantum Electronics*, *53*, pp.1-17.